Proceedings of the 28th IEEE
EMBS Annual International Conference
New York City, USA, Aug 30-Sept 3, 2006

Synthesizing panoramic radiographs by unwrapping dental CT data

Sirilawan Tohnak, Andrew Mehnert, Stuart Crozier and Michael Mahoney

Abstract—**A method for synthesizing panoramic radiographs from dental CT data is presented. The method is based on the principles of panoramic radiography with a continuously-moving rotation center. The method computes discrete pixel sums through the CT data along normals to the medial axis of the dental arch. Compared to a conventional panoramic radiograph, the method produces less geometric distortion, less blurring, and less superimposition of other structures. The method is particularly suited to forensic identification of human remains in cases where the state of degradation precludes the possibility of obtaining a conventional panoramic radiograph.**

I. Introduction

DENTAL information is widely used in forensic science to help identify human remains. It provides one of the best avenues for identification because, unlike other body parts, teeth are not easily destroyed and are highly resistant to decomposition. The forensic dentist compares the post-mortem (PM) dental information with ante-mortem (AM) dental records in an attempt to establish identity. AM dental records include x-rays (radiographs), written notes and charts from an individual's medical record. The comparison is based on several characteristics including: dental structures (including the size and shape of fillings), tooth development, periodontal disease progression, bone pathology, and some oral habits such as smoking.

At the present time dental comparison is both labor-intensive and subjective. This has motivated research into the development of methods for computed-assisted comparison. The majority of existing research [1]-[8], however, has focused on the use of conventional dental radiographs such as periapical and bitewing films, and panoramic radiographs (orthopantomography: OPG). The reason for this is that these are the most abundant source of AM data. This approach has a number of drawbacks including: (i) inherently poor image quality because of the limitations of conventional x-ray transmission radiography including: geometric distortion, difficulty distinguishing facial-oral structures, limited viewing area, and poor quality film processing; (ii) difficulty matching the viewing angles, and therefore geometry, in the PM radiographs to those used in the creation of the AM radiographs [1]; and (iii) that the quality of the human remains may preclude the possibility altogether of obtaining PM conventional radiographs or OPGs. For these reasons we propose, instead, the use of PM x-ray computed tomography (CT) data for matching against AM OPGs and conventional radiographs.

CT is a more recent, though less widely used, modality for dental imaging that does not exhibit magnification errors produced by geometric distortion [9]. Moreover, as can be seen in Fig. 1, it is a true three-dimensional (3D) imaging modality. The use of CT has been limited because of its cost and the higher dose of radiation a patient receives compared to conventional radiography. Consequently, CT images are not an abundant source of AM image data. However, PM CT data can be used to generate two-dimensional (2D) projections that mimic conventional radiographs and OPGs. This makes it possible to create projections from CT data with the same perspective as the AM radiographs and OPGs. In this paper we present our initial work on the development of an algorithm for synthesizing an OPG-like projection from CT data with reduced geometric distortion, blurring, and superimposition of other dental structures than is typically present in a real OPG.

This paper is organized as follows. Section II provides a brief overview of panoramic radiography, computed tomography, image projection and the discrete Radon transform, and introduces the proposed projection algorithm. Section III presents the results of the algorithm as applied to two spiral CT data sets from clinical dental examinations. Finally Section IV critically examines the presented work and describes future research.

II. Methods

A. Overview of panoramic radiography

In contrast to a conventional radiograph, the panoramic radiograph is acquired by rotating the x-ray tube and the film around the patient's head as shown in Fig. 2a. The process of image formation is known as tomography. Tomography, or body section radiography, is a radiographic method that allows a single layer or section of the body to be imaged whilst at the same time blurring out the shadows of superimposed structures from other layers. In the case of panoramic radiography, the curved plane in which structures are most clearly seen is called the *focal trough* or *image plane*. The x-ray tube head and the film carrier are

Manuscript received 03 April, 2006.
S. Tohnak*, A. Mehnert, and S. Crozier are with the School of Information Technology and Electrical Engineering, The University of Queensland, QLD 4072, Australia (*corresponding author: phone: +61-7-33652429, fax: +61-7-33654999; e-mail: sirilawa@ itee.uq.edu.au).
M. Mahoney is with the School of Dentistry, The University of Queensland, QLD 4072, Australia.

connected and rotate about a single point or axis called the *rotation center*. The film itself is made to move at a slower speed than the x-ray beam. This is achieved by contrary movement of the film relative to the beam [10]. The speed of the film relative to the beam is chosen such that the horizontal and vertical magnifications are equal. This occurs for only one plane, the image plane. The x-ray source emits a narrow vertical beam and as the system rotates a 2D image is exposed on the film.

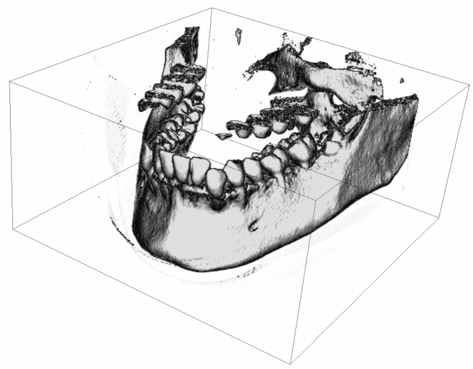

Fig. 1. A volume rendering of 3D spiral CT data from a human mandible (Patient B).

In modern panoramic x-ray machines the rotation center changes as the film and x-ray tube are rotated about the patient. The location and number of rotation centers influence the size and shape of the focal trough [11]. With a single center of rotation, the shape of the focal trough is circular. However, to accommodate the elliptical shape of the dental arches manufacturers of panoramic x-ray machines have created a variety of different rotation patterns including: multiple stationary rotation centers, a continuously moving rotation center (see Fig. 2b), and a combination of stationary and moving rotation centers [10], [11]. The shape and size of the focal trough is designed to accommodate the *average* jaw. A panoramic radiograph is shown in Fig. 3a.

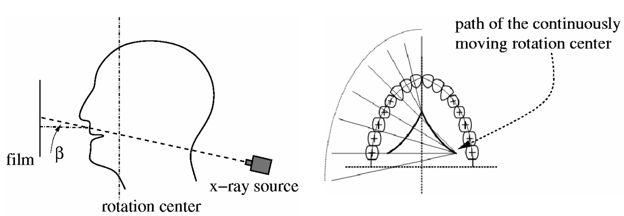

Fig. 2. (a) Geometry of panoramic radiography; (b) Example of a continuously moving rotation center pattern.

B. Computed tomography

An x-ray CT scan yields a stack of images corresponding to cross-sections or slices through the object under study. In principle the object slice data are generated by rotating the source-sensor assembly around the object, and multiple slice images are acquired by progressively moving the object through the assembly. Each CT image is a 2D matrix of grey-scale values. The matrix elements correspond to voxels rather than pixels because the slices have thickness. The grey-scale value of a given voxel represents the x-ray attenuation for that voxel; i.e. the proportion of the x-rays that are scattered or absorbed as they pass through the voxel. CT is a true 3D imaging modality. In contrast to conventional and panoramic radiography, which are 2D projections of 3D volumes, CT makes it possible to view the internal dental anatomy without the superimposition of other structures [12].

C. Image projection and the discrete Radon transform

A conventional dental radiograph fundamentally represents the summation of x-ray attenuation along each ray transmitted from the x-ray source to the film. The attenuation is due to x-ray absorption by incident bones and tissue. It follows that it is possible to emulate conventional radiographs by taking 2D projections through 3D CT data. Given that the CT data are discrete this amounts to computing finite pixel sums rather than line integrals. An important tool here is the discrete Radon transform (DRT). The DRT is a mapping from a 2D discrete function (matrix) to a set of 1D discrete projections [13]. Essentially the DRT computes multiple parallel-beam projections of the image matrix from different angles.

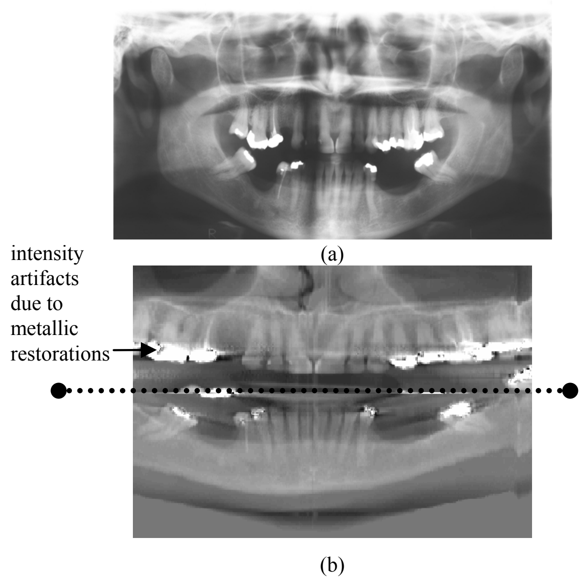

Fig. 3. Patient A: (a) OPG; (b) OPG-like projection produced by the proposed algorithm. The image is actually a composite of two separate projections. The part above the dotted line is reconstructed from the maxilla data using $\beta=0^{\circ}$. The part below the dotted line is reconstructed from the mandible data using $\beta=8^{\circ}$.

D. Proposed algorithm for synthesizing a panoramic radiograph from CT data

Our proposed algorithm generates an OPG-like image with reduced geometric distortion, blurring, and superimposition of other dental structures than is typically present in a real OPG. This is achieved by: (i) zeroing all of the voxels outside of the dental arch; (ii) tracking along the medial axis of the dental arch and projecting through the CT data normal to the tangent; and (iii) performing the projections for the left and right sides of the dental arch in isolation. The algorithm is shown in Table 2.1. The steps of the algorithm are illustrated in Fig. 4. The inputs to the algorithm are the axial CT data and a tilt angle β (see Fig. 2a). Additionally, at step 4 the user is required to manually define a contour around the dental arch to establish a mask. The aim is to define a mask that isolates the voxels of the dental arch and whose medial axis passes through the center of the arch.

TABLE 2.1

PROPOSED ALGORITHM FOR SYNTHESIZING A PANORAMIC RADIOGRAPH

Inputs: Set of axial CT slice images through the mandible or maxilla; Tilt angle β

Output: 2D panoramic image

Steps:

1. Interpolate the CT data to a cubic grid (e.g. using tricubic interpolation);
2. Rotate the volume through the angle β into the axial plane and interpolate to the grid;
3. Compute the maximum intensity projection (MIP) of the resultant set of horizontal slices (Fig. 4a);
4. Use the MIP to manually define a binary mask that corresponds to the dental arch (Fig. 4b,c);
5. For each horizontal slice image in turn, set all the pixels outside of the binary mask to zero;
6. Thin the mask [14] to obtain a single pixel medial axis (MA) (Fig. 4d);
7. Locate the end pixel of the MA corresponding to the posterior left of the dental arch;
8. For each neighboring MA pixel in turn up to the second last pixel, estimate the slope of the tangent at that pixel by computing the gradient of the line passing through its predecessor and its successor;
9. Smooth the set of angle estimates (Fig. 4e);
10. Locate the midline that divides the dental arch into two halves (Fig. 4b);
11. Locate the end pixel of the MA corresponding to the posterior left of the dental arch;
12. For each neighboring MA pixel in turn up to the midline,
    a. For each slice in turn,
        i. Create a copy of the slice;
        ii. Zero the pixel values in the copy slice that are on the opposite side of the midline;
        iii. Compute the DRT of the copy slice, centered at the MA pixel, normal to the tangent line and record only the projection corresponding to the ray passing through the pixel (Fig. 4d);
    b. Use the set of retained projections to define a column of pixels in the 2D projection image;
13. Locate the end pixel of the MA corresponding to the posterior right of the dental arch;
14. This step is identical to Step 12.

III. EXPERIMENT AND RESULTS

Two spiral CT data sets and an OPG film were used to test the algorithm (implemented in MATLAB 7, The MathWorks, Inc., Natick, MA, USA). The data originate from dental examinations performed on two patients by staff at Queensland Diagnostic Imaging. The data are summarized in Table 3.1. The maxilla CT data for Patient A were acquired parallel to the occlusal plane. The mandible CT data on the other hand were acquired at an angle to the occlusal plane. Consequently the algorithm was applied independently to the two data sets, with different tilt angles, and the results concatenated as shown in Fig. 3b. This necessarily introduces a discontinuity at the join. A comparison with the real OPG in Fig. 3a reveals that the synthesized OPG exhibits reduced geometric distortion, reduced blurring, and reduced overlapping of other dental structures. In particular, (i) horizontal magnifications in the premolar area of the synthesized OPG are less than in the real OPG, more faithfully reproducing actual proportions; (ii) the overlapping in the posterior teeth is eliminated; and (iii) the root curvature in the posterior left and posterior right are preserved. However intensity artifacts are apparent in the teeth with metallic restorations. These result from streaking artifacts manifest in the CT data (metal artifacts). The data for Patient B is of the mandible only and the slices are parallel to the occlusal plane. A volume rendering of this data is shown in Fig.1. The result of the application of the algorithm is shown in Fig. 4f. Again the synthesized OPG has less blurring, geometric distortion, and overlapping than is characteristic of a real OPG. Patient B has no dental restorations and hence there are no metal artifacts.

IV. DISCUSSION AND CONCLUSION

In this paper a novel algorithm for synthesizing panoramic radiographs from dental CT data was presented. The algorithm generates an OPG-like image with reduced geometric distortion, reduced blurring, and reduced superimposition of other dental structures than is typically present in a real OPG. More importantly, however, the algorithm permits such images to be produced from post-mortem dental CT scans. This is valuable because the state of the dental remains may preclude the possibility of obtaining actual panoramic radiographs, and indeed conventional radiographs. Given that OPGs and conventional radiographs represent the most abundant source of ante-mortem image data, the ability to synthesize an OPG from post-mortem CT data represents a significant advantage for the forensic scientist.

The results presented for Patient A demonstrate that the presence of metallic dental restorations leads to intensity artifacts in the synthesized OPG image. The attenuation of metal artifacts and beam hardening artifacts (which can compound the problem) will be the subject of future research.

This research represents part of a larger initiative to develop quantitative image analysis and pattern recognition tools to assist the forensic dentist with the task of identifying human remains by matching post-mortem CT data to ante-mortem OPGs and conventional radiographs. Future research will include the development of algorithms for synthesizing intra-oral radiographs, and the development of quantitative features (image measurements) that characterize the dental information—tooth morphology, size, dental arch characteristics, etc.—in these images and also in digitized conventional and panoramic radiographs.

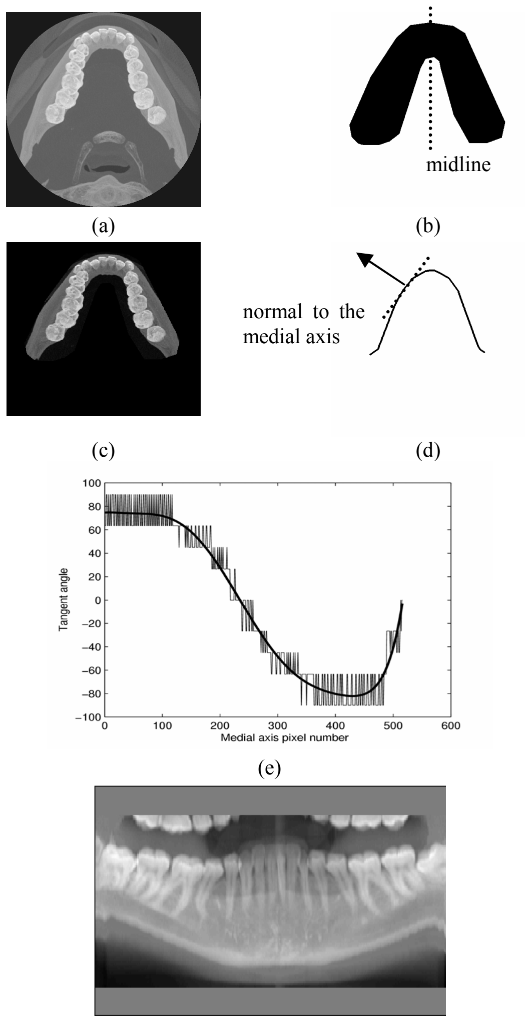

Fig. 4. Patient B: (a) Axial MIP of the CT data rendered in Fig. 1; (b) binary mask of the dental arch; (c) masked MIP image; (d) medial axis of the binary mask; (e) distribution of tangent angles along the medial axis (proceeding from left to right), with a polynomial fit (of degree 7) superimposed; (f) OPG-like projection produced by the proposed algorithm for β=0.

ACKNOWLEDGMENT

The authors would like to thank Queensland Diagnostic Imaging for providing the dental CT data and OPG film.

TABLE 3.1

DATA USED TO TEST THE ALGORITHM

	Spiral CT data	OPG film
Patient A	109 axial slices through the mandible (voxel size of 0.24 × 0.24 × 0.50 mm); 115 axial slices through the maxilla (voxel size of 0.18 × 0.18 × 0.50 mm)	Yes
Patient B	113 axial slices through the mandible (voxel size of 0.21 × 0.21 × 0.50 mm)	No

REFERENCES

[1] J. Zhou and M. Abdel-Mottaleb, "A content-based system for human identification based on bitewing dental X-ray images," *Pattern Recognition*, vol. 38, pp. 2132-2142, 2005.

[2] J. Zhou and M. Abdel-Mottaleb, "Automatic human identification based on dental X-ray images" in *Proceedings of SPIE - The International Society for Optical Engineering, Biometric Technology for Human Identification*, Orlando, FL, USA, 2004, pp. 373-380.

[3] M. H. Mahoor and M. Abdel-Mottaleb, "Classification and numbering of teeth in dental bitewing images," *Pattern Recognition*, vol. 38, pp. 577-586, 2005.

[4] O. Nomir and M. Abdel-Mottaleb, "A system for human identification from X-ray dental radiographs," *Pattern Recognition*, vol. 38, pp. 1295-1305, 2005.

[5] A. K. Jain, H. Chen, and S. Minut, "Dental Biometrics: Human Identification Using Dental Radiographs," in *Proceedings of Fourth International Conference on Audio- and Video-Based Biometric Person Authentication*, Guildford, UK, 2003, pp. 429-437.

[6] A. K. Jain and H. Chen, "Matching of dental X-ray images for human identification," *Pattern Recognition*, vol. 37, pp. 1519-1532, 2004.

[7] H. Chen and A. K. Jain, "Tooth contour extraction for matching dental radiographs," in *Proceedings of the 17th International Conference on Pattern Recognition*, Cambridge, United Kingdom, 2004, 522-525.

[8] E. Said, G. F. Fahmy, D. Nassar, and H. Ammar, "Dental X-ray image segmentation," in *Proceedings of the SPIE - The International Society for Optical Engineering, Biometric Technology for Human Identification*, Orlando, FL, USA, 2004, pp. 409-417.

[9] M. W. Vannier, C. F. Hildebolt, G. Conover, R. H. Knapp, N. Yokoyama-Crothers, and G. Wang, "Three-dimensional dental imaging by spiral CT: A progress report," *Oral Surgery, Oral Medicine, Oral Pathology, Oral Radiology, and Endodontology*, vol. 84, pp. 561-570, 1997.

[10] U. Welander, G. Tronje, and W. D. McDavid, "Theory of Rotational Panoramic Radiography," in *Panoramic Radiology*, O. E. Langland, R. P. Langlais, W. D. Mcdavid, and A. M. DelBalso, Eds., 2nd ed. Philadelphia: Lea & Febiger, 1989, pp. 38-75.

[11] W. D. McDavid, G. Tronje, U. Welander, C. R. Morris, and P. Nummikoski, "Imaging characteristics of seven panoramic X-ray units," *Dentomaxillofac Radiol*, vol. 8 (suppl), pp. 1-68, 1985.

[12] M. W. Vannier, C. F. Hildebolt, R. H. Knapp, G. Conover, N. Yokoyama-Crothers, and G. Wang. (2001,10,12). *3D dental imaging by spiral CT* [Project activities in Electronic Radiology Laboratory website].Available: http://milan.wustl.edu/PROJS/Dental/3dd_sCT.html.

[13] G. Beylkin, "Discrete Radon transform," *IEEE Transactions on Acoustics, Speech, and Signal Processing*, vol. 35, pp. 162-172, 1987.

[14] L. Lam, S.-W. Lee, and C. Y. Suen, "Thinning methodologies-a comprehensive survey," *IEEE Transactions on Pattern Analysis and Machine Intelligence*, vol. 14, pp. 869-885, 1992.